Mechanism and Kinetics of Transcellular Transport of a New β-Lactam Antibiotic Loracarbef Across an Intestinal Epithelial Membrane Model System (Caco-2)

Ming Hu,[1,3] Jiyue Chen,[1] Yanping Zhu,[1] Anne H. Dantzig,[2] Robert E. Stratford, Jr.,[2] and Mike T. Kuhfeld[2]

Received January 25, 1994; accepted May 18, 1994

Various processes involved in the transcellular transport (TT) of loracarbef (LOR) were studied in the Caco-2 cell monolayer, a cell culture model of the small intestinal epithelium. The results provide support for presence of two AP to BL peptide TT pathways in the intestinal epithelial cell monolayer (Caco-2). The H^+ gradient-dependent pathway (K_m = 0.789 mM, and J_{max} = 163 pmol/min per cm^2) is relatively "high affinity" and "low capacity" compared to H^+ gradient-independent pathway (K_m = 8.28 mM, and J_{max} = 316 pmol/min per cm^2). In addition, TT of LOR in the presence of a H^+ gradient was inhibited 77% to 88% ($p < 0.05$) by 10 mM of cephalexin, enalapril, Gly-Pro and Phe-Pro, while TT of LOR in the absence of a H^+ gradient was only inhibited 42% to 48% ($p < 0.05$) by 10 mM of Gly-Pro and Phe-Pro. Since AP uptake is H^+ gradient-dependent and saturable while the BL efflux is mostly nonsaturable and not driven by a H^+ gradient, these two transmembrane transport processes must be different, which could be the result of two different peptide carriers. In vivo, these two transport processes must have worked in concert to produce transcellular flux of loracarbef. To explain the differences between kinetic characteristics of AP uptake and TT transport, a cellular pharmacokinetic (PK) model was developed and the results indicate that the PK model appropriately described the kinetics of LOR TT. The use of this PK model may provide an additional advantage to the use of the cell culture model because kinetic parameters at both sides of the intestinal epithelial membrane may be obtained using the same preparation. Taken together, the Caco-2 model system represents an excellent model system for the study of carrier-mediated processes involved in the TT of peptides and peptide-like drugs.

KEY WORDS: transcellular transport; apical uptake; basolateral efflux; oral β-lactam; carbacephem; loracarbef; peptide carrier; H^+ gradient; cellular pharmacokinetics; transport model; Caco-2.

INTRODUCTION

Loracarbef (LOR) belongs to a new class of oral β-lactam antibiotics called carbacephem (Fig. 1). It has a chemical structure distinctively different from earlier classes of β-lactams; i.e., the dihydrothiazine ring traditionally associated with natural or semi-synthetic β-lactam is replaced by a tetrahydropyridine ring derived from total synthesis (1). As a consequence, this drug is more stable than its predecessors in solution and plasma (1). LOR represents a new and important addition to oral β-lactam antibiotics (1). While its efficacy is similar to earlier classes of β-lactam antibiotics, it has a superior safety profile in pediatric and geriatric populations (1).

Because the bioavailability of oral β-lactam antibiotics may directly affect their efficacy and safety (e.g., complete absorption lessens the chance of an unfavorable drug interaction with the intestinal microflora), pharmacokinetic parameters following oral administration of LOR have been determined (1,2). The results indicated that LOR was well absorbed in humans (approximately 100%) (2) and not metabolized, with virtually 100% of the oral dose recovered in the urine (2). Because it is charged at normal small intestinal pH, passive diffusion is an unlikely route for the absorption of this small organic zwitterion. Evidence in support of a carrier-mediated mechanism for LOR uptake into the small intestinal epithelium, as have been demonstrated for several other β-lactams (3–8), was recently reported by Dantzig and coworkers (9). It was demonstrated that LOR uptake into the Caco-2 cells was stimulated by an inwardly directed H^+ gradient and was saturable and inhibitable (9). The present report represents an extension of the work by examining the transcellular transport (TT) of LOR across the Caco-2 cell monolayers. In addition, the present study employed a new well stirred diffusion chamber and used cells grown onto porous membrane support.

The Caco-2 model represents a model of the small intestinal epithelium (10) and has been used to study the transport mechanism of several natural peptides and peptide-like drugs (9,11–15). It is an attractive system to study absorption mechanism because variables can be controlled rather precisely and easily by replacement of media at one or both sides of the monolayer. In this report, the kinetic parameters for TT, AP uptake and BL efflux of LOR were determined. The effects of various inhibitors on TT of LOR were also determined. Based on the results obtained, a cellular pharmacokinetic model for TT of LOR is proposed.

MATERIALS AND METHODS

Materials

[^{14}C]-LOR was provided by Lilly Research Laboratories (Indianapolis, IN) and was determined to be approximately 98% pure by HPLC (not shown). [H^+]-Mannitol was purchased from Dupont-NEN (Boston, MA). Cell culture supplies including media (DMEM), trypsin and N-2-hydroxyethylpiperazine-N'-2-ethanesulfonic acid (HEPES) were purchased from JRH Biosciences (Lenexa, KS). Fetal bovine serum was purchased from Hyclone Laboratories (Logan, UT), Phe-Pro, Gly-Pro, Hank's balanced salt solution (HBSS, powder form) and 2-[N-morpholino]-ethanesulfonic acid (MES) were purchased from Sigma Chem. Co. (St. Louis, MO). Cephalexin-HCl and loracarbef were provided by Lilly Research Laboratories (Indianapolis,

[1] Department of Pharmaceutical Sciences, College of Pharmacy, Washington State University, Pullman, Washington 99164-6510.
[2] Lilly Research Laboratories, Lilly Corporate Center, Indianapolis, Indiana 46285.
[3] Address correspondence to: Ming Hu, Department of Pharmaceutical Sciences, College of Pharmacy, Washington State University, Pullman, Washington 99163.

0724-8741/94/1000-1405$07.00/0

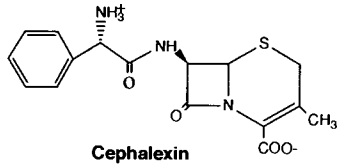

Cephalexin

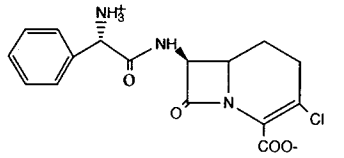

Loracarbef

Fig. 1 Structures of cephalexin and loracarbef. These structures are presented in their zwitterionic forms as existed under physiological conditions.

IN). Enalapril, enalaprilat and lisinopril, were kindly provided by Merck and Co. (West Point, PA).

Cell Culture

The Caco-2 cells, originated from Dr. J. Fogh at the Research Unit of Memorial Sloan-Kettering Cancer Center (Rye, NY), were provided by Lilly Research Laboratories (Indianapolis, IN). Cells used in the present study were from passage 33–45. Briefly, the cells were maintained in a culture flask and passed (1:10) every week. The cells were harvested at approximately 95% confluence and seeded at a density of 500,000 cells per Millicell®-PCF (30 mm diameter, 3.0 μm pore size, Millipore Corp, Bedford, MA.), and grown in DMEM media supplemented with 10% fetal bovine serum, glutamine and nonessential amino acids (10,11). The cells were fed every other day and the cell monolayers were ready to use in approximately 18 days. Cell monolayers were used between 18–24 days post seeding and 24 hr post-feeding because the transport activity was highest under these conditions (not shown). The quality of the cell monolayers was determined by measuring the transepithelial electrical resistance (TEER, normally 700–1000 ohms · cm^2) and the leakage of a paracellular transport marker, [^{3}H]-mannitol (normally $\leq$ 0.23%/hr/cm^2). The % leakage (concentration) was used here since the volume of the donor and receiver chambers is slightly different and different concentrations of mannitol may be used (see Study Protocol). Reported transport results were obtained with monolayers that had a leakage less than 0.23%/hr/cm^2. These quality control criteria are similar to those conducted in other laboratories as well as to our earlier investigations (10–14).

Study Protocol

Transport Experiments. Ordinary transport studies at 37°C without inhibitors were performed in HBSS supplemented with 20 mM of glucose, 9 mM of sodium bicarbonate, and 25 mM of HEPES for pH 7.4 buffer or 25 mM of MES for pH 6.0 buffer. A solution containing dual labeling of [^{14}C]-LOR and [^{3}H]-mannitol was used in all transport experiments while only [^{14}C]-LOR was used in uptake and efflux due to poor retention of [^{3}H]-mannitol intracellularly. The experiments were performed in triplicate using a new diffusion chamber (15). This chamber system, provides stirring by magnetic means, maintains a consistent pH, and does not result in the evaporation of media (15). Before any transport studies, a cell monolayer was washed three times with HBSS to remove the growth media, which was then followed by incubation with HBSS for one hour. For TT studies, the solution containing the compound of interest was loaded into the apical (AP) side (or AP chamber) of the monolayer, and the appearance of the compound in the basolateral (BL) (or BL chamber) media was followed by removing a 1 ml aliquot from the receiver chamber. A sample was taken every 20 or 30 min for a total of six samples and assayed according to the method described under "sample analysis." For uptake studies, the compound of interest was presented to the AP side. After a 15 min incubation, experiments were stopped and the amount of drug associated with the cell monolayer was determined. A 15 min incubation was used because amount taken up versus time was linear for up to 20 min (not shown). For efflux experiments, the cell monolayers were loaded with LOR for 1 hour at 37°C in the cell culture cluster. After the excess LOR was removed by washing with ice-cold buffer three times, monolayers were subsequently loaded into diffusion chambers and loaded LOR was allowed to efflux. The amount of drug in the BL media was measured immediately after loading, and afterwards at 5, 10, 15, 20, 30, 60, 90, and 120 min. At the end of these experiments (TT, uptake or efflux), the amounts of drug in the monolayers were determined after solubilizing the monolayers with Triton X-100. The amount of protein was assayed according to Bradford's method (16).

Inhibition Studies. A similar protocol was used to perform inhibition studies, in which a solution containing an inhibitor and LOR was placed in the AP chamber and the appearance of the drug in the BL chamber was then monitored. When high concentrations of potential inhibitors (e.g., cephalexin HCl) were used in the transport solution, the pH of the solution was always adjusted to the desired value after the compound had dissolved. Since it was not possible to perform all the inhibition experiments using the same batch of cells, a control experiment (LOR = 0.2 mM) in triplicate that measured the transport in the AP (pH 6) to the BL (pH 7.4) direction was performed for each batch of cells, and the results of inhibition experiments were always normalized to the control value. The control experiments were critical to the inter-comparability of different batches of cells since the control value may change as much as 30%.

Sample Analysis

The radiolabeled compounds were analyzed using liquid scintillation spectrophotometry (Model 2500 TR, Packard Ins. Co., Meriden, CT) with quench correction.

Data Analysis

Mannitol Leakage. Leakage was expressed as % transported/hr per cm^2. The % transported was obtained by dividing drug concentration in the receiver side with drug concentration in the donor side. The % transported was used because the volume of the received chamber is different from that of the donor chamber.

TT. A plot of amount of TT versus time was always generated following a TT experiment. Since TT was apparent linear with time after an initial lag time (see Results), flux or rate of transport (V_{TT}) was determined from linear regression analysis of amount transported versus time data. The slope of the regression curve is V_{TT} while the lag time is calculated by dividing negative Y-intercept with slope. Fluxes calculated in this way were used consistently for the purpose of presenting and comparing results. They were also used to determine the kinetic constants of the peptide carrier systems by nonlinear regression analysis of a Michaelis-Menten type equation (see equation 2) using a software program called Systat™ (Intelligent Software, Evanston, IL).

$$V_{TT} = \frac{J_{max.TT} \cdot C}{K_{m.TT} + C} + K_{TT} \cdot C \qquad (1)$$

In equation (1), $J_{max.TT}$ is the maximum rate of transepithelial transport; $K_{m.TT}$ is an apparent affinity constant; C is the concentration of the substrate in the donor compartment (e.g., AP chamber), and V_{TT} is the flux at 37°C and K_{TT} is the first-order rate constant representing the nonsaturable component of the TT process.

Intracellular Concentration. The intracellular drug concentrations at the end of a two hour experiment were determined by dividing the amount of drug inside the cells with cellular volume of 3.66 μl/mg cellular protein (9).

Uptake. Uptake was expressed as nmol/min/mg protein or nmol/min/cm^2. The uptake rate was obtained from the linear range of the amount taken up versus time curve, which was linear for up to 20 min (not shown). This uptake rate can also be used in a Michaelis-Menten type equation like equation (1) to calculate J_{max} and K_m.

Efflux. The amount of drug effluxed may be expressed as % effluxed/cm^2 versus time. This expression is used for conducting H^+ gradient-dependent efflux studies. The % effluxed/cm^2 was calculated by dividing amount effluxed (nmol) at time t with total amount of loaded drug, normalized against surface area.

The % effluxed/cm^2 was used because the amount of loaded drug in different monolayers were different depending on loading conditions (e.g., media pH). The initial rate of efflux (% effluxed/min/cm^2) was calculated by linear regression analysis of the % effluxed/cm^2 versus time plot at times less or equal to 20 min. The amount of drug left in the cell monolayers was similarly expressed as % remaining/cell monolayer at the end of efflux experiment (t = 120 min). The total amount of loaded drug was calculated by adding the amount of drug effluxed and amount remained in the cells at the end of a two hour experiment after the efflux studies were completed.

Efflux may also be expressed as pmol/cm^2 while the initial rate of efflux may be expressed as pmol/min/cm^2. This expression was used for efflux studies at different loading concentrations but with the same efflux media. These efflux rates may be used in a Michaelis-Menten type equation similar to equation (2) to calculate J_{max} and K_m.

Statistics. Statistical analyses of the data presented in the "Results" section were performed by an unpaired Student's T-test. A prior level of significance was set at 5% or $p < 0.05$. The software used was Systat™.

RESULTS

pH-Dependent Transport

Transcellular Transport. The vectorial TT of LOR (0.2 mM) was measured in the direction of AP to BL and vice versa (Fig. 2). AP to BL transport rate following a H^+ gradient (pH 6–pH 7.4) (39 ± 1 pmol/min per cm^2) was approximately five times ($p < 0.05$) as fast as the BL to AP transport rate (7.0 ± 0.1 pmol/min per cm^2) against a H^+ gradient. In addition, there was a 16 ± 3 min lag time in the AP to BL transport, compared to −8 ± 3 min for the BL to AP transport. The rate of transport of mannitol was similar in both directions (0.082 ± 0.005%/hr per cm^2 at AP to BL direction versus 0.074 ± 0.007%/hr per cm^2 at BL to AP direction). In addition to the measurement of vectorial TT of LOR with a H^+ gradient, the rates of AP to BL transport of LOR with the same pH at both sides (pH 6 or pH 7.4) of the cell monolayer were also measured (Fig. 2). The rates of TT were 15 ± 0.3 pmol/min per cm^2 at pH 6.0 and 12 ± 0.3 pmol/min per cm^2 at pH 7.4, respectively. These transport rates were approximately one-half to one-third of TT following a AP to BL H^+ gradient.

AP Uptake. Steady-State uptake of LOR was also measured under conditions identical to those shown in Fig. 2 (Fig. 2-insert). At the end of a two hour incubation period, the intracellular concentration of LOR was highest under a H^+ gradient of pH 6.0–pH 7.4 (2.1 ± 0.3 mM, 100%), followed by that without H^+ gradient at pH 6 (1.1 ± 1 mM, 50%) or at pH 7.4 (0.09 ± 0.00 mM, 5%), all of them were higher than BL uptake against a H^+ gradient (0.07 ± 0.01 mM, 3%).

BL Efflux. Release of LOR, which was loaded into the cell monolayer with 0.2 mM drug solution for 1 hr, was faster and more complete at the end of a two hour experiment with

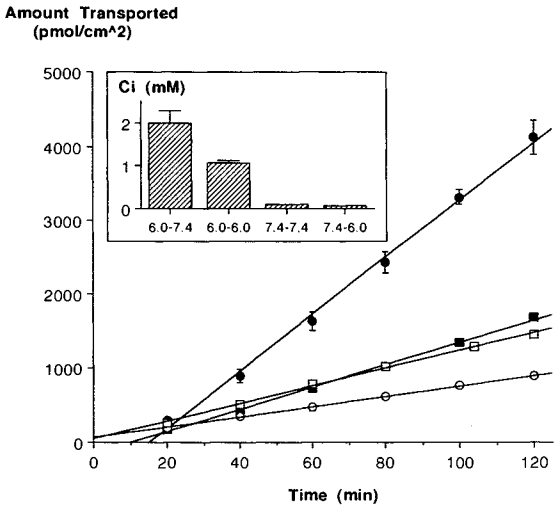

Fig. 2 Effect of time, H^+ gradient and polarity on the TT of LOR. The figure shows AP to BL TT of LOR (0.2 mM) following a transepithelial H^+ gradient (solid circles) or without a transepithelial H^+ gradient at pH 6 (solid squares) or at pH 7.4 (hollow squares) versus BL to AP TT of LOR against a transepithelial H^+ gradient (hollow circles). The insert show intracellular concentrations measured under identical conditions. Each data point represents the average of three determinations with three different monolayers and the error bar represents standard deviation of the mean.

a BL media pH of 7.4 compared to pH 6 (Fig. 3). The average initial efflux rates, calculated from the initial portion (or zero-order region) of the amount effluxed versus time plot, differed by a factor of three (0.25 ± 0.01%/min/cm^2 at pH 7.4). There was also a two fold difference in the maximum amount effluxed at the end of a two hour experiment (11 ± 0.5%/cm^2 at pH 7.4). The amount of LOR remaining in the cells, on the other hand, differed by 8 times (0.5 ± 0.07% left in the cell monolayer at pH 7.4), with much more drug remaining in the cells after an efflux experiment into a pH 6 media.

Effects of Competitive Inhibitors

AP to BL TT of LOR (0.2 mM) in the presence of a H^+ gradient was measured in the presence of an excess amount (10 mM) of Phe-Pro, Gly-Pro, cephalexin, enalapril, lisinopril, and enalaprilat. TT of LOR was inhibited significantly ($p < 0.05$) by the natural peptides Gly-Pro and Phe-Pro as well as by the peptide analogs, cephalexin, enalapril and lisinopril (Table I), but not by enalaprilat (16% reduction, $p > 0.1$). In addition, increasing concentrations of cephalexin resulted in more inhibition of LOR TT.

The effect of selected inhibitors on AP to BL TT of LOR in the absence of H^+ gradient (pH 7.4 at both sides) were also determined. The presence of 10 mM Gly-Pro or Phe-Pro caused a 42–48% reduction in TT; whereas 10 mM cephalexin or enalapril did not have any significant effect (Table I). Although the percent inhibition was less in the absence of a H^+ gradient, the absolute residual TT rates after inhibition with or without a H^+ gradient were similar.

Concentration-Dependent Transport

TT in the Presence of a H^+ Gradient. The time-dependent appearance of LOR in the BL media was measured at 37°C as a function of the AP loading concentration (0.2–7.5 mM). The appearance was linear with time after an initial lag time for all concentrations within 120 min (not shown). The lag time (T_{lag}), which was calculated by dividing negative Y-intercept with slope, decreased as the concentration increased (Table II). The rate of appearance was dependent on concentration and saturable (Fig. 4). Applying a nonlinear regression analysis to the Michaelis-Menten equation, the appearance kinetic parameters were estimated to be: K_m, 0.789 mM; J_{max}, 163 pmol/(min · cm^2); and the first-order rate constant for the nonsaturable component, 23.4 pmol/(min · cm^2 · mM) or (23.4 × 10^{-6} cm/min).

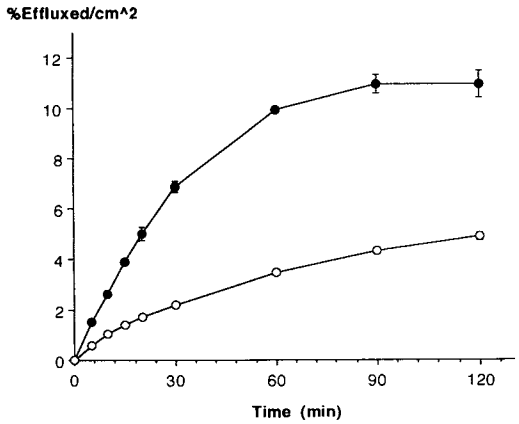

Fig. 3 Effect of BL pH on the BL efflux of LOR. The cell monolayers were first loaded with 0.2 mM of LOR for 60 min at 37°C in the presence of H^+ gradient according to procedures described in "Materials and Methods". Following a wash-off of excess LOR, the loaded LOR was allowed to efflux into a BL media containing a pH 6 buffer (hollow circles), or a pH 7.4 buffer (solid circles). Each data point represents the average of three determinations with three different monolayers and the error bar represents standard deviation of the mean.

Table I. Effect of Various Competitive Inhibitors on the AP to BL TT Rate of LOR (0.2 mM)[a]

Compound	Concentration (mM)	H^+-gradient (% control[b])	No H^+-gradient (% control[c])
Loracarbef	7.5	16 ± 3*	82 ± 12
Cephalexin	5	26 ± 2*	ND[d]
Cephalexin	10	24 ± 2*	119 ± 18
Cephalexin	20	14 ± 2*	ND[d]
Enalapril	10	21 ± 2*	84 ± 12
Lisinopril	10	75 ± 3*	ND[d]
Enalaprilat	10	84 ± 3	ND[d]
Phe-Pro	10	13 ± 2*	53 ± 2*
Gly-Pro	10	12 ± 1*	58 ± 18*

[a] A set of control experiments (LOR = 0.2 mM, 37°C) were performed for each batch of cells in the presence (pH6–pH7.4) or absence (pH7.4–pH7.4) of a H+ gradient. All results of the inhibition experiments were normalized against the control.
[b] Control value for the TT of LOR in the presence of H^+ gradient ranges from 54 ± 1 to 60 ± 3 pmol/min/cm^2 depending on the batch of cells used. Values are the average of three determinations.
[c] Control value for TT of LOR in the absence of a H^+ gradient was 7.2 ± 1.2 pmol/min/cm^2. Values are the average of three determinations. This control value was approximately 23% of TT under a H+ gradient of 6.0–7.4.
[d] Not determined.
* The star symbol indicated that there was a statistically significant difference ($p < 0.05$) between the treatment and control by Student T-test.

TT in the Absence of a H^+ Gradient. The time-dependent appearance of LOR in the BL media at different loading concentrations (0.2–15 mM) was measured, and the appearance was linear with time (not shown). However, the calculated lag time (T_{lag}) was negative at all concentration with no apparent relationship to concentration (Table II), suggesting there was minimal lag time before reaching the steady state. The appearance rates, which were also calculated as described previously, were plotted against concentrations (Fig. 5). Applying a nonlinear regression analysis to the Michaelis-Menten equation, the apparent parameters were estimated to be, K_m, 8.28 mM; J_{max}; 316 pmol/(min · cm^2); and the first-order rate constant for the nonsaturable component was 8.06 pmol/(min · cm^2 · mM) or (8.06 × 10^{-6} cm/min).

AP Uptake. The initial AP uptake rates at different concentrations were measured in the presence of an inwardly directed H^+ gradient (Fig. 6). This gradient was established

Table II. Effect of Loading Concentrations (C_o) on Lag Time (T_{lag}), Intracellular Accumulation (IA), and Intracellular Concentration (C_i) of LOR[a]

C_o (mM)	T_{lag} (min)	IA (nmol/mg protein)	C_i (mM)	C_i/C_o
Proton Gradient Present AP 6.0 → BL 7.4				
0.2	11.9 ± 1.8	4.25 ± 0.01	1.16 ± 0.01	5.8
0.5	12.6 ± 1.0	13.2 ± 0.7	3.60 ± 0.20	7.2
1	10.6 ± 1.6	34.0 ± 2.5	9.29 ± 0.68	9.3
2.5	7.6 ± 1.4	65.9 ± 1.9	18.0 ± 0.5	7.2
5	5.1 ± 1.4	106 ± 4	28.9 ± 1.1	5.8
7.5	3.8 ± 0.7	114 ± 4	31.2 ± 1.0	4.2
Proton Gradient Absent AP 7.4 → BL 7.4				
0.2	−4.9 ± 3.0	0.24 ± 0.01	0.066 ± 0.002	0.329
1	−9.2 ± 2.0	2.68 ± 0.15	0.73 ± 0.04	0.734
5	−8.3 ± 1.3	6.09 ± 0.20	1.66 ± 0.06	0.333
7.5	−8.7 ± 2.8	26.6 ± 0.1	7.28 ± 0.03	0.971
15	−9.0 ± 1.8	39.9 ± 1.34	10.9 ± 0.4	0.727

[a] Values for T_{lag}, IA and C_i represent the average of three determinations. The Ci's were calculated using the average volume of 3.66 μl/mg protein. Lag time (T_{lag}) was calculated by dividing the negative Y-intercept by the slope of the amount transported versus time curve. The values in this table were generated with two batches of cells, one for H + gradient-dependent transport, and one for H + gradient-independent transport.

by imposing a pH 6 buffer at the AP side while relying on the Caco-2 cells to maintain an intracellular pH of approximately 7.4, as shown by several laboratories (17–19). The kinetic parameters obtained were 4.32 mM for K_m, 735 pmol/(min · cm^2) for J_{max}, and 0 for the nonsaturable component, respectively.

BL Efflux. The efflux rates at several concentrations were measured in the absence of a H^+ gradient (BL pH 7.4) (Fig. 7). The Michaelis-Menten kinetic parameters for the BL efflux were obtained by fitting data to equation (1) by nonlinear regression ($R^2 > 0.99$). The estimated parameters were reported as: the K_m, 1.7 mM; J_{max}, 33 pmol/(min · cm^2); and K (first order rate constant), 3.64 pmol/(min · cm^2 · mM) or 3.64 × 10^{-6} cm/min); respectively.

H^+ Gradient- and Concentration-Dependent Accumulation

In addition to the determination of kinetic parameters of various transport processes, the intracellular concentrations (C_i) of LOR at the end of a two hour experiment were also determined as a function of applied (donor) concentration. These intracellular concentrations were calculated by dividing the amount taken up per mg protein with the amount of cellular water per mg protein, which equals to 3.66 μl per mg protein (9). The results indicated that cell monolayers were capable of concentrating LOR in the presence of an inwardly directed H^+ gradient (Table II). In contrast, in the absence of a H^+ gradient, the cells failed to concentrate LOR intracellularly (Table II). This effect of the H^+ gradient existed at all the applied concentrations, as would be expected for a saturable process. The difference in intracellular concentra-

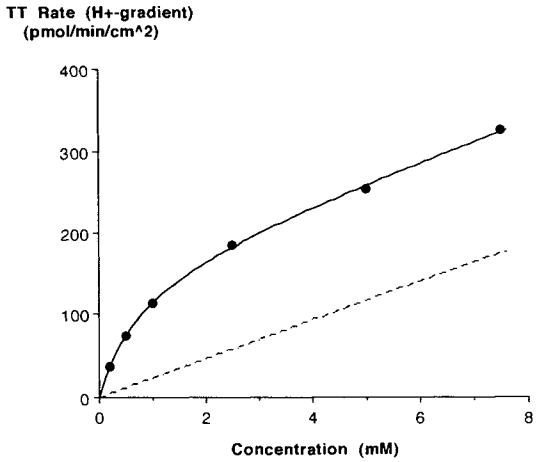

Fig. 4 Effect of concentration on the TT of LOR at 37°C in the presence of H^+ gradient. Each data point represents the average of three determinations with three different monolayers and the error bar represents standard deviation of the mean. The solid line represents the best fit line using equation (1) while the dotted line represents the nonsaturable component of TT.

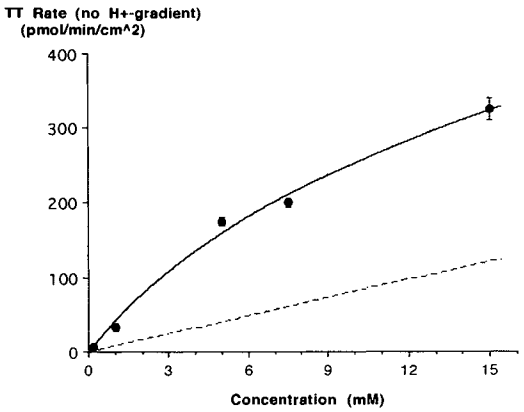

Fig. 5 Effect of concentration on the TT of LOR at 37°C in the absence of H^+ gradient. Each data point represents the average of three determinations with three different monolayers and the error bar represents standard deviation of the mean. The solid line represents the best fit line using equation (1) while the dotted line represents the nonsaturable component of TT.

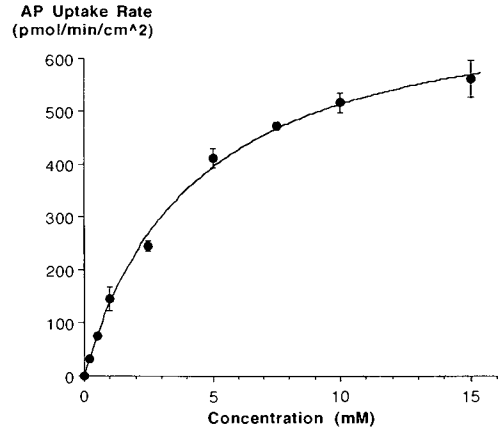

Fig. 6 Effect of concentration on the uptake of LOR at 37°C in the presence of H^+ gradient. Each data point represents the average of three determinations with three different monolayers and the error bar represents standard deviation of the mean. The solid line represents the best fit line using an equation similar to equation (1). No nonsaturable component was obtained from the fit.

tion was diminished as the applied concentration increased (Table II).

DISCUSSION

Transport Pathways

The intestinal absorption mechanisms of oral β-lactam antibiotics are well characterized. Evidence so far indicates that carrier-mediated transport is the major pathway responsible for the absorption of these drugs (5–8,20–21). There is also a general agreement regarding the existence of a AP H^+ gradient-dependent peptide carrier (the H^+ gradient theory, ref 21) in vitro and in vivo, although Matthews and coworkers reported that the bulk pH change did not affect the uptake of peptides into intestinal rings (22). However, the latter could be the result of an intestinal microclimate pH

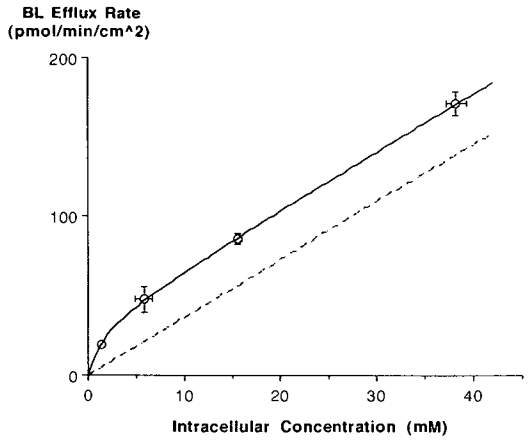

Fig. 7 Effect of concentration on the efflux of LOR at 37°C in the absence of H^+ gradient. Each data point represents the average of three determinations with three different monolayers and the error bar represents standard deviation of the mean. The solid line represents the best fit line using an equation similar to equation (1) while the dotted line represents the nonsaturable component of efflux.

that is unaffected by the change in bulk pH (24). Our results support the hypothesis that a transepithelial H^+ gradient is important for the absorption of peptide-like drugs, and that the H^+ gradient-dependent TT is the major route of transport for LOR across the intestinal epithelial membrane. These results are consistent with earlier studies of AP to BL TT of other β-lactam antibiotics in these cells (13,25). For example, Inui and coworkers have shown that the AP to BL TT of cephradine is consistently faster following a H^+ gradient than against a H^+ gradient (13).

In contrast to the H^+ gradient-dependent transport, there is no general agreement as to what is the possible contribution of a second peptide transporter to the overall transcellular process because it appears to take up substrates at a slower rate (6,23). Our studies demonstrate the H^+ gradient-independent TT pathway transports LOR at approximately one-quarter (at 0.2 mM) to one-half (at 7.5 mM) of the rates compared to H^+ gradient dependent pathway, indicating that this pathway is fairly significant. This result agrees with the report by Thwaites and coworkers who also showed a significant H^+ gradient-independent pathway (approximately 50% of H^+ gradient dependent pathway) when studying TT of Gly-Sar in the Caco-2 cell monolayers (11). Further studies are necessary to show whether the H^+ gradient-independent pathway involves a second peptide carrier and where that carrier may be located. This is because our cellular pharmacokinetic modeling (to be presented later) indicates that TT is a hybrid kinetic process whose kinetic parameters are dependent on both AP uptake and BL efflux processes.

The dependence of TT on the H^+ gradient suggest the presence of two TT pathways for LOR. To further distinguish H^+-dependent and H^+-independent pathways, TT rates of LOR (0.2 mM) were measured when different inhibitors were loaded apically in the presence or in the absence of a H^+ gradient. Enalapril and cephalexin inhibited TT only in the presence of a H^+ gradient. In contrast, Phe-Pro and Gly-Pro inhibited TT under both conditions and caused a rather complete inhibition of carrier-mediated pathway. These competition studies provide further evidence that there are two pathways for TT of LOR: one is H^+ gradient-dependent while the other is not. In addition to inhibition studies, there are also other evidence in support of the two transport pathway hypotheses: (1) kinetic parameters of TT were different in the presence versus in the absence of a H^+ gradient, i.e., the H^+ gradient-dependent TT has a relatively smaller K_m (or "high affinity") and low J_{max} (or "low capacity") compared to the H^+ gradient-independent TT; and (2) the Caco-2 cells were capable of concentrating LOR at all concentrations in the presence of a H^+ gradient but were not able to do so at any concentration tested in the absence of a H^+ gradient (Table II).

Uptake, Accumulation and Efflux

Intracellular accumulation is the net result of uptake minus efflux over a period of time (2 hr in the present study). Assuming efflux is independent of AP pH, a higher accumulation represents higher uptake. Our observation that accumulation is H^+ gradient-dependent suggest that the uptake is a H^+ gradient-dependent process, which is similar to previ-

ous observations of LOR and cephradine uptake into the Caco-2 cells (9,11). It is also consistent with the results of Thwaites and coworkers who have demonstrated that the accumulation of Gly-Sar is H^+ gradient dependent (11). In addition to H^+ gradient-dependence, the uptake was also saturable with a K_m value comparable to those obtained earlier using the same drug or other compounds (9,11–13).

Unlike uptake of peptides, there are far less BL efflux studies (11) and no kinetic parameters of transport have been reported. Because the BL efflux is the important second (or last) step in TT of LOR, we determined the effect of transmembrane H^+ gradient and intracellular LOR concentration on the BL efflux. Surprisingly, the BL efflux was faster with no H^+ gradient across the BL membrane. Furthermore, the BL efflux appeared to be mainly mediated by a nonsaturable kinetic process. This observed effect of a H^+ gradient on efflux was similar to those shown by Thwaites and coworkers (11), in which a decreased BL efflux (from 2.4 ± 0.0 nmol/h to 1.6 nmol ± 0.1 nmol/h) was the result of a decreased BL media pH, also from pH 7.4 to pH 6 (page 241, ref 11). This effect of H^+ gradient on the efflux suggest the presence of a pathway other than passive diffusion. Because BL efflux of LOR was also partially carrier-mediated (especially at lower concentration) (this study) and BL efflux of cephradine was shown to be temperature-dependent and p-chloromercuribenzene sulfonate sensitive (13), the evidence suggests that the BL efflux is at least partially via a carrier-mediated process. A carrier-mediated efflux process is also partially supported by results that showed a carrier-mediate BL uptake of peptides (12,26). Taken together, these studies indicate that AP to BL TT of LOR following a transepithelial H^+ gradient (pH 6–pH 7.4) is likely to consist of carrier-mediated AP uptake, which is energized by an inwardly directed H^+ gradient, followed by BL efflux in the absence of a H^+ gradient that is partially carrier-mediated, although not necessarily by an energy required process.

Cellular Pharmacokinetic Modeling

Although it was possible to identify two transport pathways, it is considerably more difficult to determine the relative contribution of the AP uptake process versus the BL efflux process to the overall TT process. The fact that the apparent kinetic parameters of TT did not agree with either AP or BL transport parameters (especially K_m) lead us to believe that this disparity is mainly due to the difference in the kinetic process. In other words, the steady state TT involves AP uptake followed by BL efflux, while the uptake only represents transport across a single membrane. Therefore, depending on the relative rates of these two kinetic processes, the final apparent TT rates may be quite different from the AP uptake rates.

To account for these differences, a cellular pharmacokinetic model describing the TT process and various apparent K_m's and V_{max}'s associated with different transport processes was proposed (Fig. 8). The model characterizes TT under steady-state conditions in the presence of transepithelial H^+ gradient (AP 6, BL 7.4), since cellular accumulation at the end of a one hour transport study was not different ($p > 0.25$) from that at the end of a two hour transport study (not shown). These conditions were similar to those used by

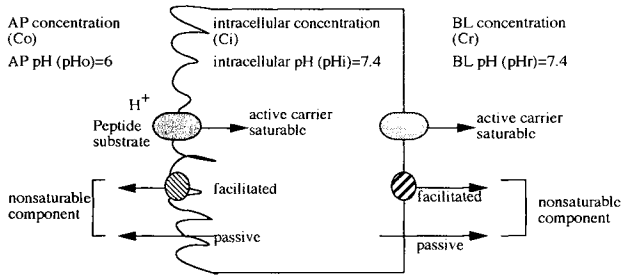

Fig. 8 A schematic representation of the cellular pharmacokinetic model under steady-state conditions.

other investigators in TT of peptides in these cells (11,12). Based on these conditions; we have derived the following equations to describe the net uptake and efflux rates under steady state conditions (See Appendix 1 for derivation).

For net AP uptake rate:

$$V_{AP.up.net} = \frac{J_{max.AP.up}\, C_o}{K_{m.AP.up} + C_o} - K_{AP.ef}(C_i - C_o) \qquad (2)$$

For net BL efflux rate:

$$V_{BL.ef.net} = \frac{J_{max.BL.ef}\, C_i}{K_{m.BL.ef} + C_i} + K_{BL.ef}\, C_i \qquad (3)$$

In equations (2)–(3), subscript "$_{AP}$" and "$_{BL}$" stand for AP and BL membranes while subscript "$_{up}$" and "$_{ef}$" stand for uptake and efflux. C_o and C_i stand for donor (AP) and intracellular drug concentration, respectively.

At steady-state, $V_{TT} = V_{AP.up.net} = V_{BL.ef.net}$. After V_{TT}, C_o and C_i were measured experimentally, the kinetic parameters were obtained from model fitting ($r^2 > 0.98$ for all the fits) (Table III). The TT rates calculated from model derived kinetic parameters provide good estimate of the experimentally measured rates (Table III). In addition, the model-derived AP uptake kinetic parameters were similar to those determined experimentally. Moreover, the model-derived BL efflux parameters were also similar to those determined experimentally. However, there were some differences between model-derived $K_{AP.up}$ (13.5 pmol/min/cm^2/mM) and experimentally determined $K_{AP.up}$ (0 pmol/min/cm^2/mM). This may be due to: (1) there was very little uninhibitable uptake (approximately 5–6% of total uptake, not shown), which may make it unaccountable; (2) some drug may leak through the paracellular pathway; and (3)

Table III. Summary of Model Derived and Experimentally Determined Kinetic Parameters

Parameters	AP uptake	BL efflux	TT
J_{max} (pmol/(min · cm^2))			
Model-derived	1031	46.0	—
Expt	735	33.3	163
K_m (mM)			
Model-derived	3.86	0.541	—
Expt	4.32	1.7	0.789
K (pmol/(min · cm^2 · mM))			
Model-derived	13.5	7.79	—
Expt	0	3.64	23.4

Table IV. Comparison of Model Derived vs Experimentally Measured TT Rates at 37°C in the Presence of a Proton Gradient

Concentration (mM)		TT rates (pmol/min/cm^2)			
C_o[a]	C_i[a]	V_{expt}[a]	V_{TT}[b]	$V_{ap.up.net}$[b]	$V_{bl.ef.net}$[b]
0.2	1.16	37.7	37.7	37.8	40.4
0.5	3.60	74.9	75.1	76.4	68.0
1	9.29	114	115	100	116
2.5	18.0	186	183	196	185
5	28.9	254	258	259	270
7.5	31.2	325	323	361	288

[a] Experimentally measured variables.
[b] Model derived variables. V_{TT} was calculated using experimentally-derived $K_{m.TT}$, $J_{max.TT}$ and K_{TT} derived from equation (1). Experimentally measured C_i's and model derived kinetic parameters (e.g., $J_{max.AP.up}$ and $K_{m.Ap.u}$) were used in the calculation of $V_{AP.up.net}$ and $V_{BL.ef.net}$ by equations (2) and (3).

first-order kinetic constants for AP uptake and AP efflux may be different. If the contribution of these factors to the overall TT of LOR can be factored out, a more accurate estimate of the transport parameters may be obtained.

In summary, the kinetic parameters generated from the cellular pharmacokinetic modeling suggest the measurement of TT rates and intracellular concentrations together with the cellular pharmacokinetic modeling provides a better alternative than measuring uptake alone because it provides us with AP uptake, BL efflux and TT parameters.

ACKNOWLEDGMENTS

Work was supported by Eli Lilly and Co.

APPENDIX I

Model Derivation

A cellular pharmacokinetic model of TT is depicted in Fig. 8. The following conditions are assumed to prevail at the steady state: (1) the amount transported versus time curve is linear; (2) the AP uptake is via a H^+ gradient dependent saturable carrier; (3) at the steady-state the "sink" condition for BL efflux is maintained because the intracellular concentration is at least 100 times higher than the drug concentration in the BL media; (4) back flux from the BL membrane is negligible because of the low BL drug concentration (C_r) (100 times less than intracellular concentration) and a unfavorable proton gradient; (5) passive transport into the cell monolayers are negligible because concentration of drug inside the monolayers were much higher than those at outside of cells; (6) H^+ gradient driven transmembrane transport of LOR may not occur against a H^+ gradient; and (7) paracellular transport is insignificant compared to a combination of passive and carrier-mediated transport.

Based on these assumptions, the uptake rates at any pH and any time assuming sink conditions at trans-side may be expressed by:

$$\text{at the AP membrane, } V_{AP.up} = \frac{J_{max.AP.up}\, C_o}{K_{m.AP.up} + C_o} + K_{AP.up}\, C_o \quad \text{(A1)}$$

$$\text{at the BL membrane, } V_{BL.up} = \frac{J_{max.BL.up}\, C_r}{K_{m.BL.up} + C_r} + K_{BL.up}\, Cr \quad \text{(A2)}$$

The efflux rates at any pH and any time assuming sink conditions at trans-side may be expressed by:

$$\text{at the AP membrane, } V_{AP.ef} = \frac{J_{max.AP.ef}\, C_i}{K_{m.AP.ef} + C_i} + K_{AP.ef.}C_i \quad \text{(A3)}$$

$$\text{at the BL membrane, } V_{BL.ef} = \frac{J_{max.BL.ef}\, C_i}{K_{m.BL.ef} + C_i} + K_{BL.ef}\, C_i \quad \text{(A4)}$$

Under steady-state conditions and in the presence of a transepithelial H+ gradient (AP 6, BL 7.4), we have following observations based on above assumptions:

1. $C_r \ll C_o < C_i$, and $pH_i \approx pH_r = 7.4$, therefore, $V_{BL.up}$ is assumed to be zero because active uptake does not work in the absence of a H+ gradient, and passive or facilitated transport may not move substrate against concentration gradient. In reality, this BL back uptake rate is typically less than 5% of BL efflux rate (27, 28).
2. $C_o < C_i$, therefore, no nonsaturable component in equation (A1) exists because passive and facilitated transport may not move substrate against a concentration gradient.
3. $pH_i > pH_o$, therefore, $V_{AP.ef} = K_{AP.ef}(C_i - C_o)$ because the saturable efflux carrier does not work against an H+ gradient. The term "$(C_i - C_o)$" is used becasue the extracellular concentration is not negligible compared to intracellular concentration (no sink conditions).

Substituting results 1–3 into equations (A1) to (A4), we have

$$V_{AP.up} = \frac{J_{max.AP.up}\, C_o}{K_{m.AP.up} + C_o} \quad \text{(A5)}$$

$$V_{BL.up} = 0 \quad \text{(A6)}$$

$$V_{AP.ef} = K_{AP.ef}(C_i - C_o) \quad \text{(A7)}$$

$$V_{BL.ef} = \frac{J_{max.BL.ef}\, C_i}{K_{m.BL.ef} + C_i} + K_{BL.ef}\, C_i \quad \text{(A8)}$$

Therefore, the net AP uptake rate, $V_{AP.up.net}$, and the net BL efflux rate, $V_{BL.e.net}$, may be described by equations (A8) and (A9):

$$V_{AP.up.net} = V_{AP.up} - V_{AP.e} = \frac{J_{max.AP.up}\, C_o}{K_{m.AP.up} + C_o} - K_{AP.ef}(C_i - C_o) \quad \text{(A9)}$$

$$V_{BL.ef.net} = V_{BL.e} - V_{BL.up} = \frac{J_{max.BL.ef}\, C_i}{K_{m.BL.ef} + C_i} + K_{BL.ef}\, C_i \quad \text{(A8)}$$

Under steady-state conditions, $V_{AP.up.net} = V_{BL.ef.net} = V_{TT}$, in which V_{TT} is the TT rate under steady-state condi-

tions. Equations (A9) and (A8) are the same as equations (2) and (3) in the main text.

REFERENCES

1. R. D. G. Cooper. The carbacephems: A new beta-lactam antibiotic class. Am. J. Med., **93(suppl 6A)**:2s–6s (1992).
2. K. A. Desante, and M. L. Zeckel. Pharmacokinetic Profile of Loracarbef. Am. J. Med., **93(suppl 6A)**:16s–19s (1992).
3. A. Tsuji, E. Nakashima, I. Kagami, and T. Yamana. Intestinal absorption mechanism of amphoteric β-lactam antibiotics I: Comparative absorption and evidence for saturable transport of amino-β-lactam antibiotics by in situ rat small intestine. J. Pharm. Sci., 70:768–771 (1981).
4. A. Tsuji, E. Nakashima, I. Kagami, and T. Yamana. Intestinal absorption mechanism of amphoretic β-lactam antibiotics II: Michaelis-Menten kinetics of cyclacillin absorption and its pharmacokinetic analysis in rats. J. Pharm. Sci., **70**:772–777 (1981).
5. A. Tsuji, T. Terasaki, I. Tamai, and H. Hirooka. H^+-Gradient-dependent and carrier-mediated transport of cefixime, a new cephalosporin antibiotic, across brush-border membrane vesicles from rat small intestine. J. Pharmacol. Expt. Ther., **241**:594–601 (1987).
6. K. Inui, T. Okano, H. Maegawa, M. Kato, M. Takano, and R. Hori. H^+-Coupled transport of p.o. cephalosporins via dipeptide carriers in rabbit intestinal brush-border membranes: difference of transport characteristics between cefixime and cephradine. J. Pharmacol. Expt. Ther. **246**:235–241 (1988).
7. P. J. Sinko and G. L. Amidon. Characterization of the oral absorption of β-lactam antibiotics. I. Cephalosporins: Determination of intrinsic membrane absorption parameters in the rat intestine in situ. Pharm. Res., 5:651–654 (1988).
8. K. Iseki, M. Sugawara, H. Saitoh, K. Miyazaki, and T. Arita. Comparison of transport characteristics of amino β-lactam antibiotics and dipeptide across rat intestinal brush-border membrane. J. Pharm. Pharmacol., **41**:628–632 (1989).
9. A. H. Dantzig, D. C. Duckworth, and L. B. Tabas. Transport mechanism responsible for the absorption of loracarbef, cefixime, and cefuroxime axetil into human intestinal Caco-2 cells. Biochim. Biophys. Acta, 1191, 7–13, 1994.
10. I. J. Hidalgo, T. J. Raub, and R. T. Borchardt. Characterization of the human colon carcinoma cell line (Caco-2) as a model system for intestinal epithelial permeability. Gastroenterology, **96**:736–749 (1989).
11. D. T. Thwaites, C. D. A. Brown, B. H. Hirst, and N. L. Simmons. H^+-Coupled dipeptide (glycylarcosine) transport across apical and basal borders of human intestinal Caco-2 cell monolayers display distinctive characteristics. Biochim. Biophys. Acta. 1151:237–245 (1993).
12. H. Saito and K. I. Inui. Dipeptide transporters in apical and basolateral membranes of the human intestinal cell line Caco-2. Am. J. Physiol. **265**:G289–G294 (1993).
13. K. Inui, M. Yamamoto, and H. Saito. Transepithelial transport of oral cephalosporins by monolayers of intestinal epithelial cell line Caco-2: Specific transport systems in apical and basolateral membranes. J. Pharmacol. Expt. Ther. **261**:195–201 (1992).
14. G. Wilson, I. F. Hassan, C. J. Dix, I. Williamson, R. Shah, M. Mackay, and P. Artursson. Transport and permeability properties of human Caco-2 cells: an in vitro model of the intestinal epithelial cell barrier. J. Control. Rel., 11:25–40 (1990).
15. M. Hu, J. Chen, D. Tran, Y. Zhu, and G. Leonardo. The Caco-2 cell monolayers as an intestinal metabolism model: Metabolism of dipeptide Phe-Pro. J. Drug Targeting, 2,79–89, 1994.
16. M. Bradford. A rapid and sensitive method for the determination of microgram quantities of protein utilizing the principles of protein-dye binding. Anal. Biochem. 72:248–254 (1971).
17. D. T. Thwaites, C. D. A. Brown, B. H. Hirst, and N. L. Simmons. Transepithelial glycylsarcosine transport in intestinal Caco-2 cells mediated by expression of H^+-coupled carriers at both apical and basolateral membranes. J. Biol. Chem. **268**:7640–42, 1993.
18. S. L. Abrahamse, R. J. Bindels, and C. H. van Os. The colon carcinoma cell line Caco-2 contains an H^+/K^+-ATPase that contributes to intracellular pH regulation. Pflugers Arch. 421:591–7 (1992).
19. A. J. M. Watson, S. Levine, M. Donowitz, and M. H. Montrose. Kinetics and regulation of a polarized Na^+-H^+ exchanger from Caco-2 cells, a human intestinal cell line. Am. J. Physiol. **261**:G229–G238 (1991).
20. T. Okano, K. Inui, H. Maegawa, M. Takano, and R. Hori. H^+-coupled uphill transport of aminocephalosporins in rat intestinal brush-border membrane vesicles. Role of dipeptide transport system in rabbit intestinal brush-border membranes. J. Biol. Chem. **261**:14130–14134 (1986).
21. V. Ganapathy and F. H. Leibach. Is intestinal peptide transport energized by a H^+ gradient? Am. J. Physiol. **249**:G153–G160 (1985).
22. D. M. Matthews and D. Burston. Uptake of a series of neutral dipeptides including L-alanyl-L-alanine, glycylglycine and glycylsarcosine by hamster jejunum in vitro. Clin. Sci., **67**:541–549 (1984).
23. M. Sugawara, T. Toda, K. Iseki, K. Miyazaki, H. Shiroto, Y. Kondo, and J. Uchino. Transport characteristics of cephalosporin antibiotics across intestinal brush-border membrane in man, rat and rabbit. J. Pharm. Pharmacol., 44**(12)**:968–972 (1992).
24. T. Iwatsubo, Y. Miyamoto, Y. Sugiyama, H. Yuasa, and T. Iga. Effects of potential damaging agents on the microclimate-pH in the rat jejunum. J. Pharm. Sci., 75**(12)**:1162–1165 (1986).
25. J. Chen, Y. Zhu, A. H. Dantzig, R. E. Stratford, Jr., M. Hu. Transcellular transport of cephalexin in Caco-2 cell monolayers. Pharm. Res. S181, 1993.
26. J. Dyer, R. B. Beechey, J. P. Gorvel, R. T. Smith, R. Wootton, and S. P. Shirazi-Beechey. Glycyl-L-proline transport in rabbit enterocyte basolateral membrane vesicles. Biochem. J., **269**:565–571 (1990).
27. M. Hu and R. T. Borchardt. Transport of a Large Neutral Amino Acid in a Human Intestinal Epithelial Cell Line (Caco-2): Uptake and Efflux of Phenylalanine. Biochim. Biophys. Acta, **1135**, 233–244 (1992).
28. J. Chen, Y. Zhu, and M. Hu. Mechanisms and Kinetics of Uptake and Efflux of L-Methionine in an Intestinal Epithelial Model (Caco-2). J. Nutr, accepted.